A THERMAL-PIEZORESISTIVE SELF-SUSTAINED RESONANT MASS SENSOR WITH HIGH-Q (>95k) IN AIR

Aojie Quan[§], Chen Wang[§] , Hemin Zhang, Michel De Cooman, Chenxi Wang, Linlin Wang, Sina Sadeghpou, and Michael Kraft*

ESAT-MNS, KU Leuven, Leuven 3001, Belgium

ABSTRACT

This paper demonstrates, for the first time, a high sensitivity mass sensor based on thermal-actuation piezoresistive-detection coupled resonators with a self-sustained oscillation. In-plane-vibration resonators are actuated by thermal expansion and contraction of the nanobeams, while the vibration displacements are detected by changes in resistance. Due to the combination of the negative piezoresistive coefficient of the phosphorus-doped structural silicon layer and the thermal expansion/contraction effect, a constant direct current (DC) through the nanobeam produces a periodic resistance variation in the beam at the fundamental modal frequency as the resonator, thus a self-sustained oscillation is generated. An ultra-high quality factor of ~95k in air is obtained. Linear response with respect to mass perturbations for both amplitude ratio (of the two coupled resonators) and frequency shift readouts are observed from the proposed self-oscillating, mode-localized mass sensor. The measured sensitivity of the amplitude ratio (~162 ppm/pg) is 100 times higher than that of a shift in the normalized resonant frequency.

KEYWORDS

Self-oscillation; Coupled resonators; Mass sensor; Quality factor; Thermal-piezoresistive

INTRODUCTION

Microelectromechanical resonators have been widely applied for many sensing applications [1]. Classically, MEMS resonant sensors measure external physical quantities by a shift in their resonant frequency, which is determined by the inherent physical parameters, i.e. effective mass and stiffness. For a resonant mass sensor, the frequency shift is proportional to the mass perturbation, i.e., $\Delta f/f_0 = \delta m/2m_0$ [2]. The main challenges that such conventional resonant mass sensors face are to optimize the resolution, sensitivity, effective quality factor in the medium of a fluid and to realize a closed-loop oscillator for real-time monitoring.

For high sensitivity, mode localization of weakly coupled resonators using amplitude ratio as a readout metric is a promising approach and has already been demonstrated [3]. Generally, a mass perturbation to one resonator of the coupled resonator system causes a structural asymmetry and energy confinement [3]. This can be measured by detecting a change in the ratio of the resonant amplitudes of the two coupled resonators. Additionally, mode-localized sensors are relatively immune to environmental fluctuations, such as ambient temperature or pressure variations [4]. However, most mass sensors based on coupled resonators utilize capacitive or piezoelectric actuation/sensing. They often suffer from a low quality factor when operating in a fluid (gas or liquid) due to viscous damping. Sealed microchannel resonators have been successfully used for liquid particle sensing applications [5] and diamond has been suggested as the resonating material for high quality factor [6], albeit only for frequency shift resonators and at the cost of added fabrication complexity. For closed-loop oscillation, the classical method is to employ a phase-lock-loop (PLL) which tracks the phase of the resonator and controls the loop phase error via a PID controller; however, this requires complicated control and interface electronics and is sensitive to temperature variations.

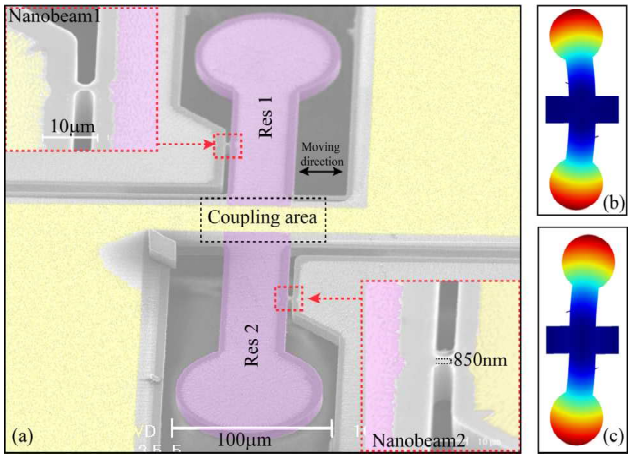

Figure 1: False-color SEM images (a) and FEM simulation of the in-phase (b) and out-of-phase (c) working modes of the coupled resonators. The yellow area is a Au/Cr multi-layer (100 nm) and forms electrodes for actuation and detection with low contact resistance.

Recently, it was shown that a thermal-piezoresistive effect can increase the quality factor of a resonator to relatively high values (>10k) [7]. Furthermore, employing the same effect, a self-sustained oscillation is possible if materials with a negative piezoresistive coefficient are used. This is due to a combination of thermal-expansion and contraction [8][9] and can significantly decrease the complexity of the interface electronics as alternating current (AC) electrical signals and phase tracking are no longer required. The self-sustained oscillation ensures that the operating frequency always corresponds to the resonant frequency of the resonators.

In this paper, we describe a DC-driven, thermal-actuation piezoresistive-detection self-sustained resonant mass sensor using mode-localization. The sensor operates in air with a quality factor as high as 95k and shows a high sensitivity. This tackles three key objectives for resonant mass sensors: high sensitivity, high Q-factor in air and self-oscillation in a single device. After tuning the coupled resonators to an appropriate working point, two different output metrics (amplitude ratio and frequency shifts) for the same mass perturbations are demonstrated and compared.

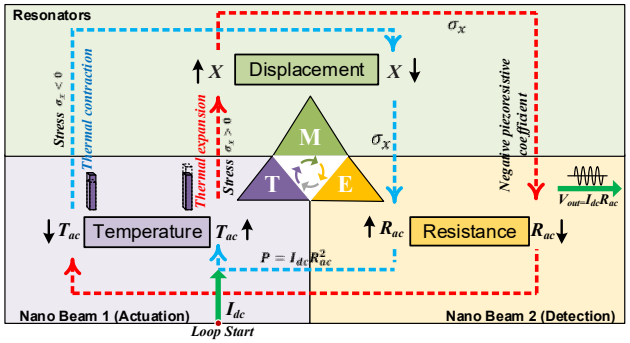

Figure 2: The thermal(T)-electric(E)-mechanical(M) interaction and self-sustained loop schematic of the self-sustained oscillator.

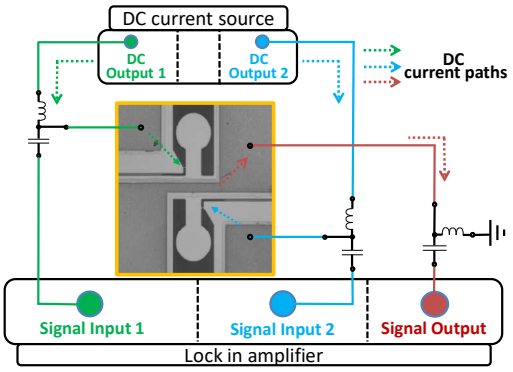

Figure 3: Electrical setup for working point tuning test.

DESIGN AND METHOD

Device description

The proposed device has a symmetric design with two thermal-actuation piezoresistive-detection resonators, which are mechanically coupled via a suspended coupling area (in Fig. 1(a)). A silicon on insulator (SOI) wafer with a heavy phosphorus-doped device layer of 9 µm thickness was used for fabrication; this has the required negative piezoresistive coefficient. For each resonator, a nanoscale beam with a width of 850 nm and a length of 5 µm links the resonator to the anchor area. The nanobeams are used as thermal actuator and piezoresistive sensors.

Self-sustained oscillation

An illustration of the working principle of the self-sustained oscillation is shown in Fig. 2. Referring to the labels of Fig. 1, a DC current 1 (I_{dc1}) is forced through nanobeam 1 causing power dissipation due to resistive Joule heating, which results in a temperature increase ($T_{ac}\uparrow$) and thus thermal expansion of the beam. This moves Res 1 away from the anchor in an axial direction of the nanobeam ($X_{ac}\uparrow$). The beam will undergo an over-expansion because of the inertia of Res 1. At the same time, the resistance of the beam decreases ($R_{ac}\downarrow$) due to tensile stress and the negative piezoresistive coefficient of the N-type silicon, thus the heat dissipation will decrease and the temperature of the beam will also decrease ($T_{ac}\downarrow$). Therefore, the beam starts contracting and pulling Res 1 back towards the anchor ($X\downarrow$). The compressive force on the beam will then increase the resistance ($R_{ac}\uparrow$), hence increase the heat dissipation and temperature ($T_{ac}\uparrow$) and push Res 1 again away from the anchor; in this way the cycle starts again.

The voltage drop across the nanobeams is an AC signal with an amplitude proportional to the varying resistance of the beam and thus also to the displacement of the resonators, therefore it provides a mean to monitor the vibration amplitudes of the resonators. Since the two resonators are physically coupled, they exhibit two fundamental in-plane resonant frequencies, as shown in Fig. 1(b) and 1(c). An oscillation of Res 2 is induced through the physical coupling from Res 1. The displacement of Res 2 can be detected by the voltage drop across nanobeam 2.

Mode-localization based sensors

For a 2-degree-of-freedom (2-DOF) coupled resonator system with amplitude ratio output, the normalized sensitivity to mass perturbation is given by:

$$\hat{u} = \left|\frac{u_i - u_0}{u_0}\right| \approx \left|\frac{K}{4K_c} \times \frac{\Delta m}{m}\right| \qquad (1)$$

where $\hat{u}$, Δm, m, K, are amplitude ratio, mass perturbation, total mass, stiffness of both resonators, respectively, and K_c is the coupling stiffness. It can be shown that the normalized sensitivity of a 2-DOF resonator system is improved by a factor of $\frac{K}{4K_c}$ compared to a conventional frequency readout [10].

EXPERIMENTAL RESULTS

Working point tuning

In order to characterize the resonant frequency of the coupled resonators, an open-loop frequency sweep was first carried out by actuating the resonators with a combination of a DC bias and an AC signal. As equation (2) indicates, when choosing an AC component with an amplitude much smaller than DC component, the term at 2ω becomes negligible.

$$P = \frac{(V_{ac} sin\omega t + V_{dc})^2}{R} = \left[\frac{V_{ac}^2 + 2V_{dc}^2}{2R}\right] + \left[\frac{2V_{ac}V_{dc} sin\omega t}{R}\right] - \left[\frac{V_{ac}^2 cos2\omega t}{2R}\right] \qquad (2)$$

where P, V_{ac}, V_{dc}, ω and R are power, AC, DC supplied voltages, angular velocity and total resistance of the resonators, respectively.

Due to fabrication tolerances, the device is not exactly identical to the layout. The fabrication errors lead to an initial asymmetry between the two resonators, leading to mode-localization and energy confinement even without applying changes in mass. Thus, the initial operating point should be tuned to ensure the sensor is in its linear region [11]. To demonstrate the principle of the operation we first introduced a stiffness perturbation by applying a variable DC current through nanobeam 2, as shown in Fig. 3. The middle part of the coupled resonator device is grounded through an inductor. Current flows through the two nanobeams; their magnitude can be controlled independently by two DC sources. A 100 mV AC frequency sweep signal (1.26 MHz to 1.29 MHz) was applied to the middle electrode from the signal output. A two-channel lock-in amplifier was used to detect the alternating voltage signals across the two nanobeams.

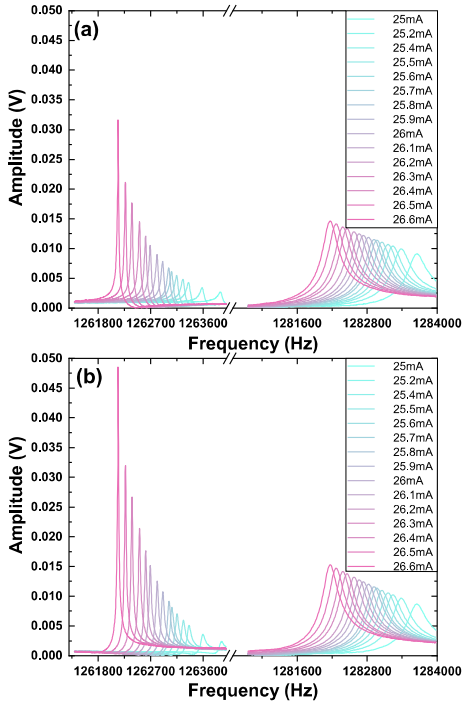

Figure 4: Frequency responses of Res 1 (a) and Res 2 (b) for different currents flowing through Res 2. The maximum quality factor was ~20k in air for the working mode (out-of-phase mode), when there is no self-oscillation.

The measured frequency responses of Res 1 and Res 2 are shown in Fig. 4. There are two distinguishable vibration modes for each resonator as predicted by the FEM simulations (see Figs. 1(b) and (c)). The resonant frequencies of the out-of- and in-phase modes are 1.26 MHz and 1.28 MHz, respectively which are close to the simulated results (1.31 MHz and 1.32 MHz).

When changing the DC current through nanobeam 2 from 25 mA to 26.6 mA while keeping the DC current through nanobeam 1 constant at 27 mA, the resonant frequencies of both modes of the two resonators decreased due to the negative elastic constant temperature coefficient of the material. With this setup the two nanobeams experience different heating powers; nanobeam with higher temperature thus creates a stiffness perturbation making the coupled resonator system asymmetric, therefore the amplitude ratio and working point is tunable.

Mass sensing with self-sustained oscillation

The test configuration of the self-oscillated mass sensor is shown in Fig. 5. The middle electrode of the coupled resonators is grounded. The values of the current flowing through the two nanobeams are controlled by the two channels of a DC current source separately, to facilitate aforementioned tuning method. The amplitudes of the AC voltage signals across the nanobeams were detected in the frequency domain by the lock-in amplifier.

As shown in Fig. 5(a), when the DC currents 1 and 2 reach 27 mA and 26.8 mA, respectively, the coupled resonators start self-oscillating and generate sinusoidal output voltages. The output amplitude from Res 1 exhibits an exponential increase and stabilizes after ~ 900 ms. The ring down response test in Fig. 6(b) indicates a quality factor of ~95,000 in air.

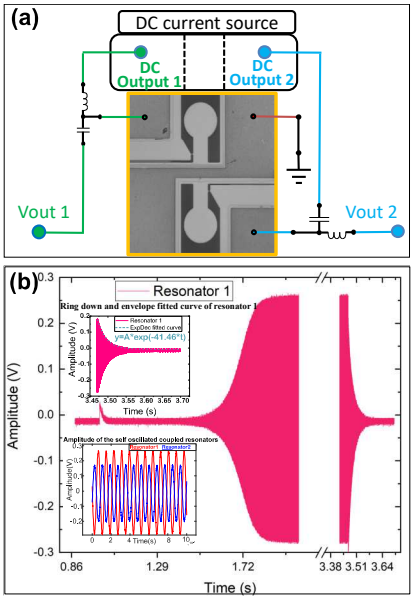

Figure 5: Test configuration of the self-oscillated mass sensor (a) and the output amplitude of the coupled resonators when starting and stopping self-oscillation in the time domain. The inset figures in (b) show the outputs of resonators 1 and 2 when the self-oscillation becomes stable and the ring-down test when decreasing the DC output 2 from 27 mA to 26.6 mA, respectively.

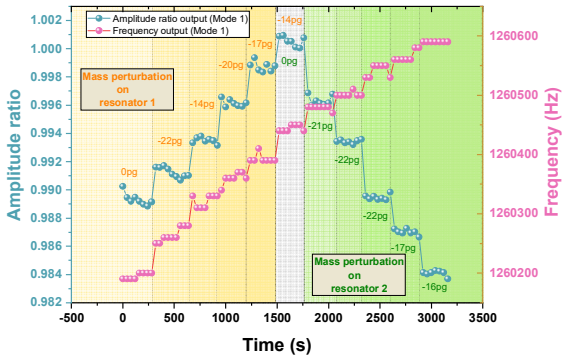

Figure 6: Mass perturbation responses of the amplitude ratio and frequency in the time domain. The orange and green areas refer to removing mass from Res 1 and Res 2, respectively; the mass is estimated by measuring the profile of bombarded surface with a phase-shifting interferometer. For every mass perturbation, 7~8 times of responses are measured in 280 s ~ 320 s intervals.

The concept of the mass sensing is validated by introducing a mass perturbation by removing first mass from Res 1 by subsequnt laser bombardments and then by Res 2 by the same method (see Fig. 7). The amplitude ratio is calculated by dividing the amplitudes of the voltages across the two resonators. Before the mass perturbation experiment, the amplitude ratio was set to approximately unity by adjusting the two DC currents.

Figure 6 shows the mass perturbation responses of the amplitude ratio and frequency in the time domain. As expected, the frequency increases when removing mass from the coupled resonators. However, an increase in the amplitude ratio only occurs when mass is removed from Res 1. In contrast, when removing mass from Res 2, the amplitude ratio drops. It can also be seen that there is a

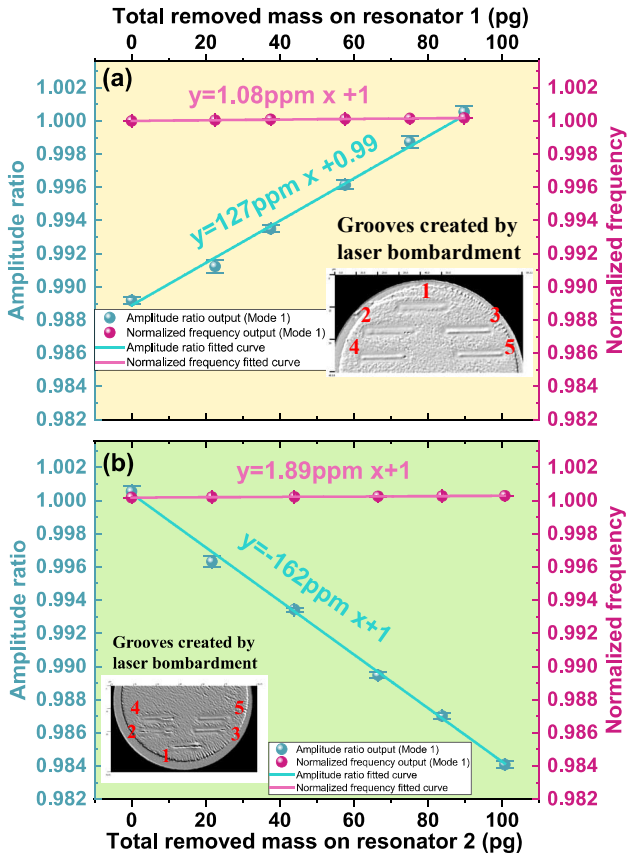

Figure 7: The amplitude ratio and normalized frequency of the coupled resonators as a function of the mass perturbations applied on Res 1 (a) and Res 2 (b). The inset pictures were taken under an optical profilometer and show the grooves created by the laser bombardments.

slight drift both for amplitude ratio and frequency output signals in a measurement interval; this is attributed to the atmospheric test environment in which small dust particles adhere to the surface and also temperature fluctuations.

The dependency of the amplitude ratio and normalized frequency with respect to the mass perturbations on the two resonators are shown in Fig. 7(a) and (b), respectively. It can be seen that both amplitude ratio and normalized frequency follow a linear trend with respect to mass perturbations. Slopes of fitting curves indicate that the sensitivity of the amplitude ratio is ~100 times higher than the typical frequency shift sensing principle. The sensitivities of the amplitude ratio and normalized frequency readouts both increase when removing mass from Res 2, which can be explained by the setup of actively driving only one resonator [12].

CONCLUSIONS

In summary, this paper demonstrates the first self-oscillated mass sensor with thermal actuation and piezoresistive sensing, and mode-lcocalization of the coupled resonators. The experimental results show that the device can be driven by a constant current with 95,000 quality factor in air. The sensitivity based on the amplitude ratio is around 100 times higher than the normalized resonant frequency while working in a self oscillation operation mode. The stability and resolution of the self-oscillated mass sensor will be examined in future work.

ACKNOWLEDGEMENTS

This work was partially supported by China Scholarship Council (CSC) grant, FWO-project grant G091220N and European Union's Horizon 2020 research and innovation programme under the Marie Skłodowska-Curie IF grant agreement No. 840165.

REFERENCES

[1] R. Abdolvand, B Bahreyni, JEY Lee, F Nabki., "Micromachined resonators: A review", Micromachines, vol. 7, no. 9, 2016.

[2] K. Ekinci, Roukes, "Nanoelectromechanical systems", *Rev. Sci. Instrum.*, vol. 76, no. 6, pp. 1–12, 2005.

[3] C. Zhao, M. H. Montaseri, G. S. Wood, S. Hui, A. A. Seshia, and M. Kraft, "A review on coupled MEMS resonators for sensing applications utilizing mode localization", *Sensors Actuators A. Phys.*, vol. 249, pp. 93–111, 2016.

[4] P. Thiruvenkatanathan, J. Yan and A. A. Seshia, "Common mode rejection in electrically coupled MEMS resonators utilizing mode localization for sensor applications", *IEEE Int. Freq. Control* pp. 358–363, 2009.

[5] T.P. Burg, M.Godin, S.M. Knudsen, W. Shen, G. Carlson, J. S. Foster, K. Babcock S. R. Manalis, "Weighing of biomolecules, single cells and single nanoparticles in fluid", *Nature*, vol. 446, no. 7139, pp. 1066–1069, 2007.

[6] V. Kara, Y. I. Sohn, H. Atikian, V. Yakhot, M. Loncar, K. L. Ekinci., "Nanofluidics of single-crystal diamond nanomechanical resonators", *Nano Lett.*, vol. 15, no. 12, pp. 8070–8076, 2015.

[7] C. S. Li, M. H. Li, C. C. Chen, C. H. Chin, and S. S. Li., "A low-voltage CMOS-microelectromechanical systems thermal-piezoresistive resonator with Q > 10,000", *IEEE Electron Device Lett.*, vol. 36, no. 2, pp. 192–194, 2014.

[8] P. G. Steeneken, K. L. Phan, M. J. Goossens, G. E. J. Koops, G. J. A. M. Brom, C. V. D. Avoort & J. T. M. V.Beek, "Piezoresistive heat engine and refrigerator", *Nat. Phys.*, vol. 7, no. 4, pp. 354–359, 2011.

[9] A. Rahafrooz, S. Pourkamali, "Thermal-piezoresistive energy pumps in micromechanical resonant structures", *IEEE Trans. Electron Devices*, vol. 59, no. 12, pp. 3587–3593, 2012.

[10] M. Spletzer, A. Raman, A. Q. Wu, X. Xu, R. Reifenberger,, "Ultrasensitive mass sensing using mode localization in coupled microcantilevers", *Applied Physics Letters*, vol. 88, no. 25. 2006.

[11] H. Zhang, B. Li, W. Yuan, M. Kraft, H. Chang, "An acceleration sensing method based on the mode localization of weakly coupled resonators", *J. Microelectromech. Syst.*, vol. 25, no. 2, p. 286, 2016.

[12] H. Zhang, H. Chang, and W. Yuan, "Characterization of forced localization of disordered weakly coupled micromechanical resonators", Microsystems & Nanoengineering., vol. 3, no. 1, pp. 17023, Jul. 2017.

CONTACT

*Hemin Zhang, hemin.zhang@kuleuven.be

§A. Quan and C. Wang contributed equally.